PROCEEDINGS OF SCIENCE

Two- and three-particle Bose-Einstein correlations in small collision systems at LHCb

Miłosz Zdybał[a,*] **on behalf of the LHCb Collaboration**

[a] *Institute of Nuclear Physics Polish Academy of Sciences,*
Radzikowskiego 152, 31-342 Kraków, Poland

E-mail: milosz.zdybal@cern.ch

The new results on three-pion Bose-Einstein correlations measured with the sample of proton–proton collisions recorded at a centre-of-mass energy of $\sqrt{s} = 7$ TeV are presented, being the first study of three-particle Bose-Einstein correlations in the forward region provided by the LHCb detector. The results are interpreted within the core-halo model for the first time in proton-proton collisions. Together with previous LHCb results on two-pion Bose–Einstein correlations measured for the first time in the forward rapidity region at LHC energies, this confirms the observation of collective phenomena in small collision systems. Moreover, the results of the three-particle analysis indicate, for the first time, coherent particle emission.

The European Physical Society Conference on High Energy Physics (EPS-HEP2025)
7-11 July 2025
Marseille, France

*Speaker

https://pos.sissa.it/

PoS(EPS-HEP2025)230

1. Introduction

Intensity interferometry provides a means to determine experimentally the properties of particle-emitting sources [1]. Boson interferometry offers insight into the space-time structure of particle production in the process of hadronisation, helping to determine the size, shape, and lifetime of the hadronisation volume. This is possible because of Bose-Einstein correlations (BEC) between pairs and triplets of identical bosons that occur for pions created close together in phase space. In this case, their quantum wave functions interfere constructively, which manifests itself in an increased probability of observing particles with a small difference in four-momentum. The study of the parameters of the density function in the region of small four-momentum difference can reveal the space-time properties of the hadron-emission volume. Analysis of two-body correlations between identical pions allows calculation of the apparent radius of the source as well as the strength of the correlation. Three-body correlations can expand this with information about thermalisation and coherence in the source.

2. Two-particle correlation function

The correlation function of two indistinguishable particles is usually studied using the Lorentz-invariant variable Q[1], related to the difference in four-momenta k_1 and k_2:

$$Q \equiv \sqrt{-(k_1 - k_2)^2} = \sqrt{M^2 - 4m^2}, \tag{1}$$

for particles with rest mass m and invariant mass M. The two-particle correlation function is defined as the ratio of the Q distributions of the signal and reference pairs:

$$C_2(Q) \equiv \frac{\rho_2(Q)^{\mathrm{sig}}}{\rho_2(Q)^{\mathrm{ref}}} = \left(\frac{N^{\mathrm{ref}}}{N^{\mathrm{sig}}}\right)\left(\frac{\mathrm{d}N^{\mathrm{sig}}(Q)\,/\,\mathrm{d}Q}{\mathrm{d}N^{\mathrm{ref}}(Q)\,/\,\mathrm{d}Q}\right), \tag{2}$$

where $\rho_2(Q)^{\mathrm{sig}}$ is the Q distribution of the same-sign particle pairs, and $\rho_2(Q)^{\mathrm{ref}}$ represents the distribution in the reference sample, which has no BEC effect. N^{sig} and N^{ref} denote the numbers of signal and reference pairs, respectively, obtained from the integrals of the corresponding Q distributions. The reference sample is intended not to include any BEC effect; in this case, this is achieved by constructing the pairs, using particles originating from different events in the event-mixing method [2]. To ensure that the kinematic distributions between the signal and reference samples agree, reference pairs are selected from events with a similar number of tracks reconstructed in the vertex detector.

When considering static, univariate sources, the two-body correlation function can be parametrised with the Lévy-type function [3]:

$$C_2(Q) = N(1 + \lambda_2 e^{-(RQ)^{\alpha_{\mathrm{L}}}})(1 + \delta Q). \tag{3}$$

The value of the parameter R can be interpreted as the radius of the spherically symmetric emission volume; the intercept parameter λ_2 (also referred to as the correlation strength) denotes the extrapolated value of the correlation function at $Q = 0$ GeV [4]; the parameter δ corresponds to long-range momentum correlations; N is the normalisation factor. The value of the Lévy index of stability, α_{L}, is set according to the assumed density distribution [3] and can take values in the range $(0, 2]$.

PoS(EPS-HEP2025)230

A *double ratio* technique is commonly used in BEC analyses to mitigate unwanted effects present in the data. These include effects related to imperfections in the reference sample construction, single-particle acceptance and efficiency, detector occupancy, selection cuts, long-range correlations, and other well-simulated phenomena. In the final fit, a ratio of correlation functions for data and simulation is used:

$$r_{\mathrm{d}}(Q) \equiv \frac{C_2^{\mathrm{data}}(Q)}{C_2^{\mathrm{sim}}(Q)}. \tag{4}$$

It is important to use the same set of selection parameters for both samples and to ensure that the simulated sample has the BEC effect turned off.

3. Correlation function for proton-lead

The parametrised correlation function for proton–lead collisions includes electromagnetic effects and the non-femtoscopic background, using the Bowler–Sinyukov formalism [5, 6] with Lévy parametrisation:

$$C_2(Q) = N\left[1 - \lambda + \lambda K(Q) \times \left(1 + e^{-|RQ|}\right)\right] \times \Omega(Q), \tag{5}$$

where $K(Q)$ corresponds to the Coulomb interactions and $\Omega(Q)$ to the non-femtoscopic background. The latter contribution was investigated using the correlation function for opposite-sign pions. The non-femtoscopic background can be described using a Gaussian parametrisation of the cluster contribution [7], as discussed in [8].

4. Three-particle correlation function

The three-particle correlation function is defined, similarly to the two-particle case, as the ratio of the three-particle four-momentum distribution to the product of one-particle distributions

$$C_3(k_1, k_2, k_3) \equiv \frac{N_3(k_1, k_2, k_3)}{N(k_1)N(k_2)N(k_3)}, \tag{6}$$

with the assumption of properly symmetrised plane waves for the wave functions and Lévy distributions as the source function, the correlation function can be expressed as a convolution of two-particle functions for all possible pairs of particles in the triplet [3, 9]:

$$\begin{gathered} C_3^{(0)}(Q_{12}, Q_{13}, Q_{23}) = C_2^{(0)}(Q_{12}) C_2^{(0)}(Q_{13}) C_2^{(0)}(Q_{23}) = \\ 1 + \ell_3 e^{-0.5[(Q_{12}R)^{\alpha_{\mathrm{L}}} + (Q_{13}R)^{\alpha_{\mathrm{L}}} + (Q_{23}R)^{\alpha_{\mathrm{L}}}]} + \ell_2 \left[e^{-(Q_{12}R)^{\alpha_{\mathrm{L}}}} + e^{-(Q_{13}R)^{\alpha_{\mathrm{L}}}} + e^{-(Q_{23}R)^{\alpha_{\mathrm{L}}}}\right], \end{gathered} \tag{7}$$

with the Lévy index of stability α_{L} fixed to 1, where ℓ_2 and ℓ_3 are parameters related to the strengths of two- and three-particle correlations.

5. Core-halo model

The region of pion emission created in the proton-proton collision can be classified as a system with a large halo [10]. In this case, the pion emission source is divisible into two distinct parts. In the central *core*, particles are created in the process of hydrodynamic evolution or particle production from excited strings, followed by rescattering. The core is surrounded by the *halo* of pions emitted from the decay of long-lived hadronic resonances (ω, η, η', K^0) with decay lengths exceeding 20 fm. The core-halo model introduces parameters that describe the characteristics of hadron emission.

The fraction of the core, f_c, denotes the proportion of particles emitted from the core of the system. The partial coherence parameter, p_c, expresses the ratio of particles emitted coherently. These two parameters can be used to express the correlation strengths λ_2 and λ_3 [4]:

$$f_c^2[(1-p_c)^2 + 2p_c(1-p_c)] = \lambda_2, \tag{8}$$

$$2f_c^3[(1-p_c)^3 + 3p_c(1-p_c)^2] + 3f_c^2[(1-p_c)^2 + 2p_c(1-p_c)] = \lambda_3. \tag{9}$$

The value of λ_2 is taken from the two-pion BEC analysis [11], while λ_3 is calculated using the fitted parameters. These measured parameters can be used to solve eq. 8 and eq. 9 for f_c and p_c.

An observable κ_3 (eq. 10) can be introduced [9] that is a function of λ_3 and λ_2. It is independent of the fraction of particles originating from the core and can be used to infer whether additional effects are present in the core, such as partial coherence or a not fully thermalised core – this would be indicated by the value of κ_3 deviating from unity.

$$\kappa_3 = 0.5(\lambda_3 - 3\lambda_2)/\lambda_2^{3/2} \tag{10}$$

6. Dataset and selection

The presented analyses of proton–proton collisions are performed using no-bias and minimum-bias triggered events collected in 2011 at a centre-of-mass energy of $\sqrt{s} = 7$ TeV. The simulation sample is prepared using Pythia 8 with a specific LHCb configuration, without a BEC effect. Events are divided into three bins of charged-particle multiplicity in the VELO detector, corresponding to different levels of event activity: low (5–10), medium (11–20) and high (21–60).

For the proton–lead analysis, a dataset of minimum-bias triggered events collected in 2013 at a nucleon–nucleon centre-of-mass energy of $\sqrt{s_{NN}} = 5.02$ TeV, with beam energies of 4 and 1.58 TeV, respectively, is used. Both beam modes, *p*Pb and Pb*p*, are employed to study collisions in the forward and backward rapidity regions. The dataset is divided into 18 bins of reconstructed charged-particle multiplicity in the VELO detector. The binning is designed to provide a sufficient number of bins with enough events to enable a measurement.

7. Two-pion Bose-Einstein correlations in proton-proton collisions

Double ratios of the correlation function were fitted in bins of charged-particle multiplicity according to Eq. 3. The results of the fits are shown in Fig. 1. The calculated parameter values corresponding to the correlation radius R and the intercept parameter λ_2 are shown in Fig. 2.

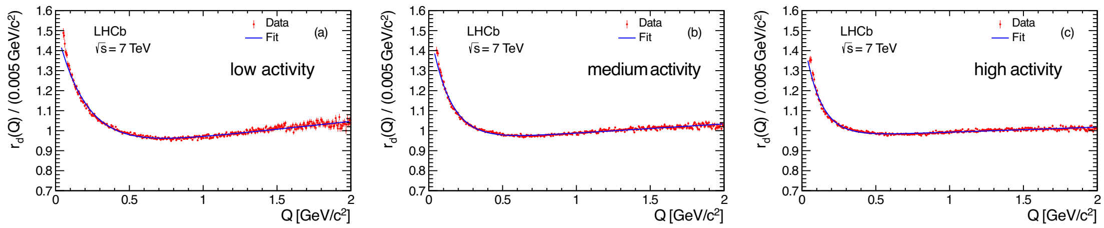

Figure 1: Results of the fit to the double ratio of the correlation function for the pion pairs for the three activity classes.

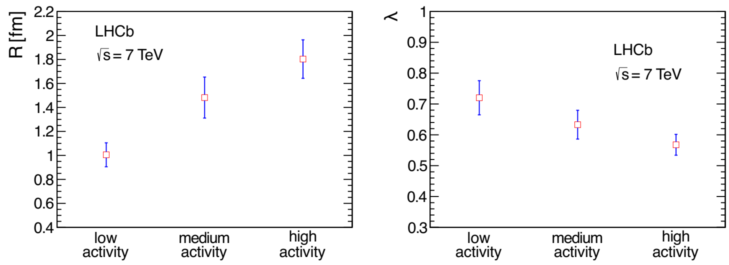

Figure 2: Correlation radius R and intercept parameter λ as functions of the reconstructed charged-particle multiplicity measured in the pp [11], pPb, and Pbp collision systems.

8. Two-pion Bose-Einstein correlations in proton-lead and lead-proton collisions

The correlation parameters were calculated by fitting the same-sign correlation functions in each bin of reconstructed charged-particle multiplicity using Eq. 5. Parameters related to the cluster contribution and background scaling were determined in previous steps of the analysis. Example results of the fits to the correlation functions are shown in Fig. 3. The behaviour of the measured correlation parameters is consistent with observations by other LHC experiments: the correlation radius increases with event multiplicity, and the intercept parameter exhibits the opposite behaviour.

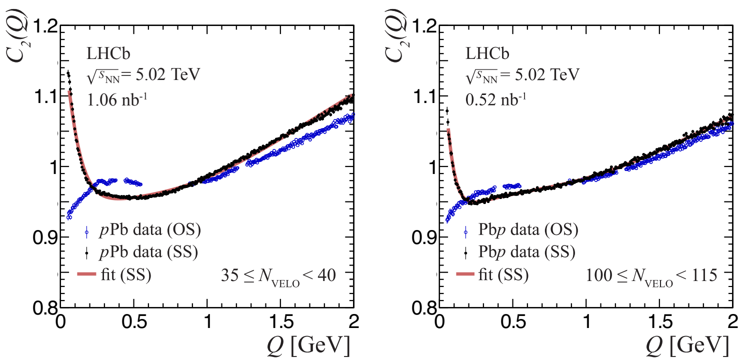

Figure 3: Selected fits to the SS correlation function are shown for a moderate-multiplicity region ($35 \leq N_{\text{VELO}} < 40$) of the pPb (left) and for a high-multiplicity region ($100 \leq N_{\text{VELO}} < 115$) of the Pb$p$.

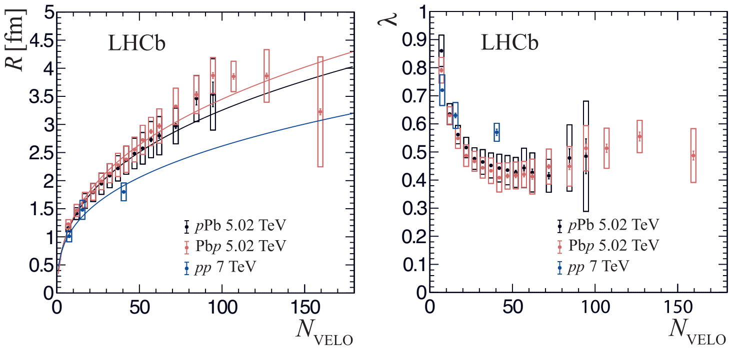

Figure 4: Correlation radius R and intercept parameter λ as functions of the reconstructed charged-particle multiplicity measured in the pp [11], pPb, and Pbp collision systems. Statistical uncertainties are indicated with error bars, while systematic uncertainties are shown with boxes. Data points are positioned at the centres of the multiplicity bins.

9. Three-pion Bose-Einstein correlations in proton-proton collisions

The results of the fit to the double ratio of correlation functions for triplets of pions are shown in Figure 5. The fits are performed for three bins of the reconstructed charged-particle multiplicity in the VELO detector.

The dependence of the calculated core–halo parameters on the charged-particle multiplicity bins is shown in Figure 6. The fraction of the core, f_c, does not show a strong dependence on the number of produced charged particles, decreasing only slightly for higher multiplicities. The behaviour of the parameter κ_3 is similar, remaining consistent with unity within statistical and systematic uncertainties. The partial coherence parameter, p_c, however, increases significantly for higher multiplicities, indicating the presence of coherent emission.

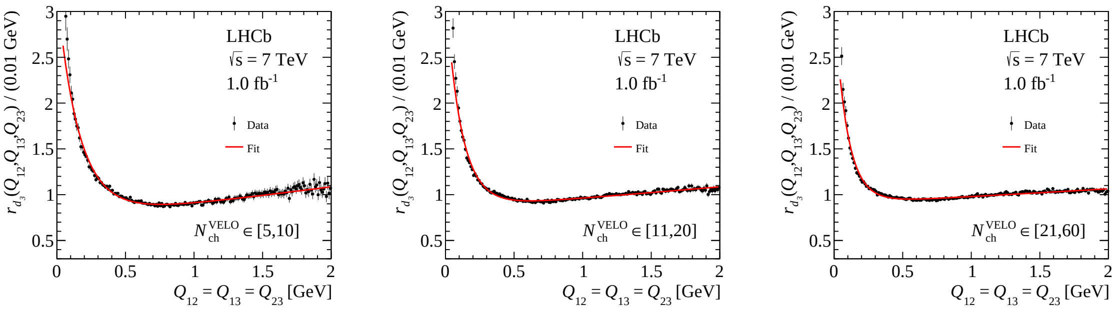

Figure 5: Results of the fit to the three-particle double ratio (r_{d_3}) for same-sign pion triplets. The red line illustrates the fit performed using the parametrisation outlined in Eq. 7.

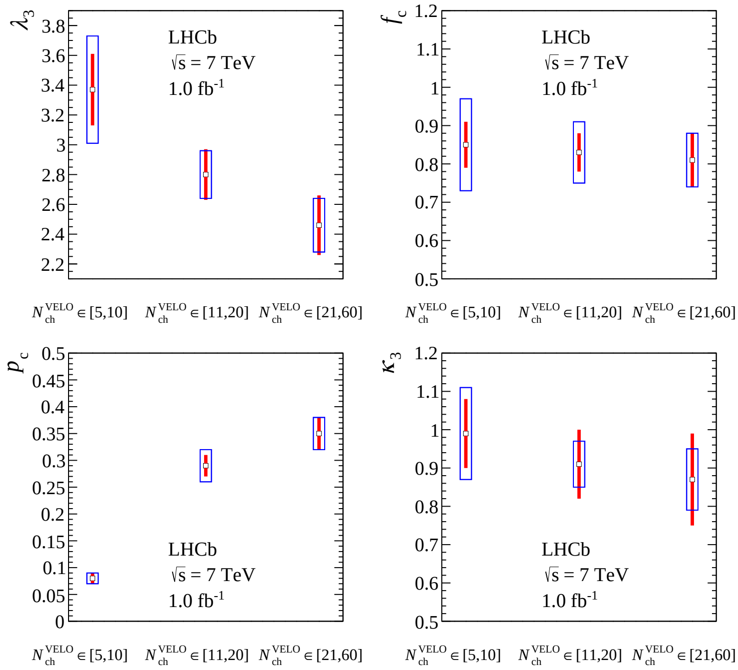

Figure 6: Values of correlation strength λ_3 and the parameters of the core-halo model determined for three bins of VELO track multiplicity. Statistical and systematic uncertainties are marked with red and blue bars, respectively.

10. Conclusions

The presented results summarise studies of Bose–Einstein correlations in small collision systems performed by the LHCb experiment. The measured parameters for the pion pairs are in agreement with previous observations by LEP [12] and other LHC experiments [7, 13–15], with values slightly lower than those reported by the ATLAS experiment for similar multiplicities. The measured correlation radius for the pPb collisions scale with the cube root of the charged-particle multiplicity, which is compatible with predictions based on hydrodynamic models. The values measured for the different beam directions show a difference, that hints at a potential sensitivity to the rapidity. The calculated values of the core–halo model parameter p_c indicate a partially coherent emission of the pions, which has not been observed before. All of the above measurements are performed for the first time in the forward region of pseudorapidity offered by the LHCb experiment, thereby broadening the understanding of the hadronisation process in small collision systems.

References

[1] G. Baym, *The physics of Hanbury Brown–Twiss intensity interferometry: from stars to nuclear collisions*, Acta Phys. Polon. B29 (1998) 1839

[2] Gideon Alexander, *Bose–Einstein and Fermi–Dirac interferometry in particle physics*, Rept. Prog. Phys. 66 (2003) 481

[3] T. Csorgo, S. Hegyi, W. A. Zajc, *Bose-Einstein correlations for Levy stable source distributions*, Eur.Phys.J. C36 (2004) 67-78

[4] T. Csorgo, *Particle interferometry from 40 MeV to 40TeV*, Nato Science Series C: Math. and Phys. Sci. 554 (2000) 203

[5] M.G. Bowler, *Coulomb corrections to Bose-Einstein correlations have been greatly exaggerated*, Phys. Lett. B 270 (1991) 69

[6] Y. Sinyukov et al., *Corrections for interferometry analysis of expanding hadron systems*, Phys. Lett. B 432 (1998) 248

[7] CMS Collaboration, *Bose-Einstein correlations in pp, pPb, and PbPb collisions at* $\sqrt{s_{NN}} = 0.9 - 7$ *TeV*, Phys. Rev. C 97, 064912

[8] LHCb Collaboration, R. Aaij et al., *Study of the Bose-Einstein correlations of same-sign pions in proton-lead collisions*, JHEP 09 (2023) 172

[9] T. Novák, *PHENIX results of three-particle Bose–Einstein correlations in* $\sqrt{S_{NN}} = 200$ *GeV Au+Au collisions*, Universe 2018, 4(3), 57

[10] T. Csorgo, B. Lorstad, J. Zimanyi, *Bose-Einstein Correlations for Systems with Large Halo*, Z. Phys. C71, 491 (1996)

[11] LHCb collaboration, R. Aaij et al., *Bose–Einstein correlations of same-sign charged pions in the forward region in pp collisions at* $\sqrt{s} = 7$ *TeV*, JHEP 12 (2017) 025

[12] OPAL Collaboration, G. Alexander et al., *Multiplicity dependence of Bose-Einstein correlations in hadronic* Z^0 *decays*, Z. Phys. C 72 (1996) 389

[13] ALICE collaboration, *Femtoscopy of pp collisions at* $\sqrt{s} = 0.9$ *and* 7 *TeV at the LHC with two-pion Bose-Einstein correlations*, Phys. Rev. D 84 (2011) 112004

[14] CMS Collaboration, *First measurement of Bose-Einstein correlations in proton-proton collisions at* $\sqrt{s} = 0.9$ *and* 2.36 *TeV at the LHC*, Phys. Rev. Lett. 105 (2010) 032001

[15] ATLAS Collaboration, *Two-particle Bose-Einstein correlations in pp collisions at* $\sqrt{s} = 0.9$ *and* 7 *TeV measured with the ATLAS detector*, Eur. Phys. J. C 75 (2015) 466